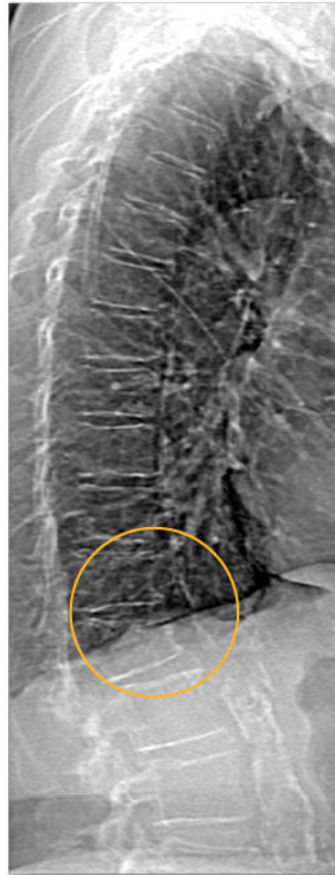


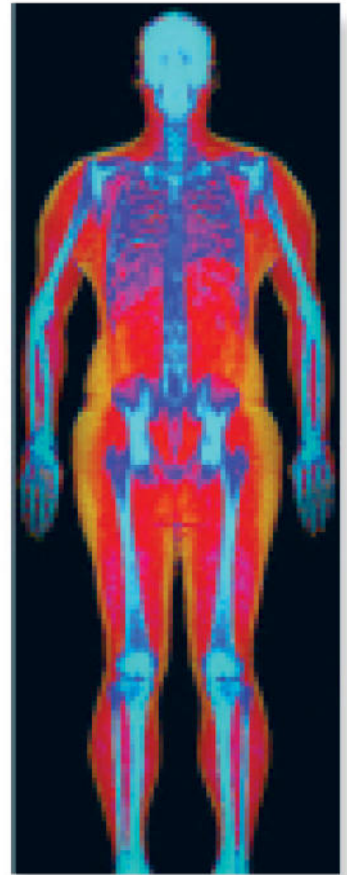
Powerful images. Clear answers.



Manage Patient's concerns about
Atypical Femur Fracture*



Vertebral Fracture Assessment –
a critical part of a complete
fracture risk assessment



Advanced Body Composition®
Assessment – the power to
see what's inside

Contact your Hologic rep today at BSHSalesSupportUS@hologic.com



PAID ADVERTISEMENT

*Incomplete Atypical Femur Fractures imaged with a Hologic densitometer, courtesy of Prof. Cheung, University of Toronto

ADS-02018 Rev 003 (10/19) Hologic Inc. ©2019 All rights reserved. Hologic, Advanced Body Composition, The Science of Sure and associated logos are trademarks and/or registered trademarks of Hologic, Inc., and/or its subsidiaries in the United States and/or other countries. This information is intended for medical professionals in the U.S. and other markets and is not intended as a product solicitation or promotion where such activities are prohibited. Because Hologic materials are distributed through websites, eBroadcasts and tradeshows, it is not always possible to control where such materials appear. For specific information on what products are available for sale in a particular country, please contact your local Hologic representative.

www.hologic.com | dxaperformance.com | 1.800.442.9892

Irisin Prevents Disuse-Induced Osteocyte Apoptosis

Giuseppina Storlino,^{1†} Graziana Colaianni,^{1†} Lorenzo Sanesi,¹ Luciana Lippo,¹ Giacomina Brunetti,² 
Mariella Errede,² Silvia Colucci,² Giovanni Passeri,^{3#} and Maria Grano^{1#} 

¹Department of Emergency and Organ Transplantation, University of Bari, Bari, Italy

²Department of Basic Medical Sciences, Neuroscience and Sense Organs, University of Bari, Bari, Italy

³Department of Medicine and Surgery, University of Parma, Parma, Italy

ABSTRACT

Previous results showed that intermittently administered irisin improves bone mass in normal mice and prevents the development of disuse-induced osteoporosis and muscular atrophy in hindlimb-suspended mice, a murine model able to mimic the absence of mechanical loading. A recent study showed that irisin increases survival of osteocytes acting through integrin $\alpha V/\beta 5$ receptors. To better understand the action of irisin on these cells, we investigated the downstream signaling cascades in osteocyte-like cells (MLO-Y4) treated with recombinant irisin (rec-irisin) in vitro and we analyzed survival of osteocytes and caspase activation in cortical bone of osteoporotic mice treated with rec-irisin in vivo. Our results revealed that rec-irisin activated the MAP kinases Erk1 and Erk2 and increased the expression of the transcription factor *Atf4* (2.5-fold, $p < .05$) through an Erk-dependent pathway in osteocytes. Some key genes expressed by MLO-Y4 cells were modulated by long-term irisin treatment, either continuously administered or given with intermittent short pulses. Interestingly, *Sost* mRNA was severely downregulated only upon intermittent irisin administration (10-fold, $p < .001$). Furthermore, rec-irisin upregulated *Tfam* mRNA (fourfold, $p < .05$) and *Bcl2/Bax* ratio (twofold, $p < .05$) in MLO-Y4 cells. By detecting caspase-9 and caspase-3, we also found that rec-irisin inhibited apoptosis induced by hydrogen peroxide and dexamethasone, respectively. In cortical bone of unloading C57BL6 mice treated with vehicle (unload-veh), irisin prevented disuse-induced reduction of viable osteocytes (+30% versus unload-veh, $p < .05$) and increase of empty lacunae (+110% versus unload-veh, $p < .05$), as well as caspase-9 (threefold, $p < .05$) and caspase-3 (twofold, $p < .05$) activations. Our findings revealed underlying mechanisms of irisin action on osteocytes, which increases their functions and exerts anti-apoptotic effects, confirming that mechanosensor cells of bone are sensitive to the exercise-mimetic myokine irisin. © 2019 American Society for Bone and Mineral Research.

KEY WORDS: ANABOLICS; BONE-MUSCLE INTERACTIONS; IRISIN; OSTEOCYTES; OSTEOPOROSIS

Introduction

Osteocytes are derived from terminally differentiated osteoblasts integrating over time into the bone matrix and networking extensively with each other through their long cellular processes that travel within narrow canaliculi. Representing about 90% of the bone cells, osteocytes play a pivotal role in communication with the cells on the bone surface and exert a control function within the remodeling unit.⁽¹⁾ Osteocytes can regulate osteoclast activity by balancing secretion of osteoprotegerin (OPG) and receptor activator of nuclear factor κ -B ligand (RANKL), and osteoblast differentiation and function by interfering with the Wnt/ β -catenin signaling through production of the Wnt antagonists sclerostin and dickkopf-1 (Dkk1).⁽¹⁾ Therefore, because the survival of osteocytes is crucial in maintaining bone

mass and function, numerous molecules (eg, cytokines, hormones) designed to prevent their apoptosis are continuously being studied by the scientific community. Glucocorticoid treatment and sex steroid deficiency have been shown to increase osteocyte apoptosis in animals and humans.^(2,3) Moreover, the osteocyte death observed in the murine model of estrogen deficiency, temporally and spatially coupled to increased bone resorption, has been shown to resemble that observed in a murine model of disuse-induced bone loss.⁽⁴⁾ Conversely, intermittent administration of parathyroid hormone (PTH) or estrogen replacement therapy prevents osteocyte apoptosis, suggesting that the anabolic action of these treatments is also exerted by preserving osteocyte survival.^(5,6) Physical activity could also promote osteocyte viability independently from fluid movement in the canaliculi resulting from mechanical loading. For instance, the exercise-induced myokine β -aminoisobutyric

Received in original form July 19, 2019; revised form November 29, 2019; accepted December 4, 2019. Accepted manuscript online December 11, 2019.

Address correspondence to: Maria Grano, PhD, Department of Emergency and Organ Transplantation, University of Bari, Piazza Giulio Cesare 11, 70124 Bari, Italy. E-mail: maria.grano@uniba.it

Additional Supporting Information may be found in the online version of this article.

[†]GS and GC contributed equally as first authors.

[#]GP and MG contributed equally as last authors.

Journal of Bone and Mineral Research, Vol. 00, No. 00, Month 2019, pp 1–10.

DOI: 10.1002/jbmr.3944

© 2019 American Society for Bone and Mineral Research

acid (BAIBA) protects osteocytes against ROS-induced apoptosis and prevents both bone and muscle loss.⁽⁷⁾ Noteworthy, it has been recently shown that another myokine, irisin, inhibited hydrogen peroxide-induced apoptosis in the MLO-Y4 (osteocyte-like) cell line.⁽⁸⁾

Irisin, a myokine released by skeletal muscles upon muscle contraction, has been shown to exert anabolic effects in several tissues, highlighting the importance of physical activity to delay the onset of age-related diseases.

We previously showed that irisin administered intermittently in healthy mice improves bone mass and its geometric, structural, and biomechanical properties.⁽⁹⁾ *in vivo* data showed higher expression of activating transcription factor 4 (*Atf4*) in bone marrow of irisin-treated mice, suggesting a substantial commitment of osteoblast precursors toward osteogenesis. The direct action of irisin on the bone-forming cells was also confirmed *in vitro*. MAP kinase Erk phosphorylation is stimulated within 5 min of irisin administration, and *Atf4* and *Collagen* mRNA expressions are upregulated in osteoblasts treated with irisin.⁽⁹⁾

More recently, we found that intermittent administration of irisin in hindlimb-suspended mice prevents the development of both disuse-induced osteoporosis and muscular atrophy. As a potential mechanism by which irisin counteracts bone loss, molecular studies have shown that in cortical bone of unloaded mice treated with irisin, sclerostin levels are maintained at the level of normally ambulating control mice, whereas the absence of load increased its expression.⁽¹⁰⁾ Recently, Kim and colleagues⁽⁸⁾ identified integrin $\alpha V/\beta 5$ as the receptor for irisin on osteocytes, paving the way to research on its downstream signaling cascades and the biological effects of irisin on these cells.

In this work, we show that irisin acts on osteocytes by increasing the expression of the transcription factor *Atf4* through an Erk-dependent pathway. We also show that long-term irisin treatment, either continuously administered or given intermittently with short pulses, modulates key genes expressed by osteocytes. Strikingly, sclerostin expression is downregulated only following intermittent administration. Moreover, we identify some apoptotic signals inhibited by irisin, which exerts pro-survival action on osteocytes in cortical bone of both aged and hindlimb-suspended mice. These data identify underlying mechanisms of irisin action on osteocytes and might encourage studies of irisin therapeutics for the treatment of bone diseases.

Materials and Methods

Cell culture

Mouse osteocytes MLO-Y4 (Kerafast, Inc., Boston, MA, USA) were used for *in vitro* experiments in this study. One-hundred millimeter \times 20-mm (100-mm \times 20-mm) plates (Corning, Corning, NY, USA) were coated with collagen (0.15 mg/mL) (Sigma-Aldrich, St. Louis, MO, USA) for 1 hour under a sterile tissue culture hood at room temperature. After coating, plates were washed with PBS (Gibco, Thermo-Fisher, Waltham, MA, USA), as described.⁽¹¹⁾ Cells were plated at 10×10^3 cells/cm² and cultured in α -MEM (Gibco, Thermo-Fisher, Waltham, MA, USA) with 10% of fetal bovine serum (FBS) (Gibco, Thermo-Fisher, Waltham, MA, USA) to maintain differentiation in a humidified atmosphere (37°C, 5% CO₂), (Hera cell 150; Thermo-Fisher, Waltham, MA, USA). As described in the supplier's datasheet (Kerafast, Inc.), criteria for MLO-Y4 cells are high osteocalcin, high Podoplanin, and low alkaline phosphatase expressions. However, we also detected *Sost* mRNA expression (average Ct:

29 cycles), as well as sclerostin protein expression (Supplementary Fig. 1B) in MLO-Y4 osteocytic cells.

To investigate the mechanism underlying the activation of osteocytes, MLO-Y4 cells were starved for 1 hour and subsequently stimulated with recombinant irisin (rec-irisin) (100 ng/mL) for 0, 1, 5, 10, 20, and 60 min. At the end of the various time points, cell cultures were lysed for immunoblot analysis of Erk phosphorylation. To evaluate the role of Erk activation in *Atf4* mRNA upregulation, MLO-Y4 cells were pretreated with 50 μ M of PD98059 (Sigma-Aldrich), a specific Erk1/Erk2 inhibitor, 20 min before stimulation with rec-irisin for 8 hours (AdipoGen Life Sciences, Liestal, Switzerland).

MLO-Y4 were treated for 6 days with continuous or intermittent pulses of rec-irisin. For continuous protocol, the medium with irisin (100 ng/mL) was refreshed every 48 hours for three times. For intermittent protocol, MLO-Y4 were treated with irisin (100 ng/mL) for 3, 8, or 24 hours. After each treatment-pulse, the medium was changed, and the procedure repeated every 48 hours for three times. To validate the experiment, we have preliminarily evaluated by ELISA assay (AdipoGen Life Sciences) whether rec-irisin administered to MLO-Y4 cells is preserved in culture for up to 48 hours (Supplementary Fig. 1A).

To identify a possible role of irisin in apoptosis, MLO-Y4 cells were treated with irisin (100 ng/mL) for 8 hours or 24 hours. For 24-hour treatments, MLO-Y4 cells were pretreated for 2 hours with 30 μ M and 600 μ M H₂O₂ (Sigma-Aldrich) or stimulated with 1 μ M dexamethasone (Sigma-Aldrich) 6 hours before the end of irisin treatment.

Animal models

Two-month-old mice C57BL6 male mice ($n = 24$) were randomly assigned to three groups: two of hindlimb-suspended mice (vehicle-injected [veh-inj] and irisin-injected [irisin-inj]) and one of control mice (rest veh-inj). Hindlimb-suspended mice were subjected to the tail suspension procedure, according to recommendations by Wronski and Morey-Holton.⁽¹²⁾ Hindlimb-suspended mice were adjusted to prevent any contact of the hindlimbs with the cage floor, resulting in approximately a 30-degree head-down tilt. The forelimbs of the animals were in contact with the cage bottom, allowing the mice full access to the entire cage. Each mouse was singly housed, maintained under standard conditions on a 12 hour/12 hour light/dark cycle and with access to water and regular diet *ad libitum* (Harlan Teklad 2019; SDS Special Diets Services, Witham, UK).

Hindlimb-suspended mice were treated with vehicle (physiologic solution sterilized by 0.22 μ filtration) ($n = 8$) or with 100 μ g/kg rec-irisin (Adipogen International, San Diego, CA, USA) ($n = 8$) by intraperitoneal injection (i.p.) once a week for 4 weeks. The group of control mice ($n = 8$) was also singly housed and received vehicle by i.p. injection once a week for 4 weeks.

Eighteen-month-old mice C57BL6 male mice (old mice, $n = 16$) were randomly assigned to two groups: one group ($n = 8$) treated with vehicle, and the other ($n = 8$) treated with 100 μ g/kg rec-irisin by i.p. injection once a week for 4 weeks. Old mice were singly housed, maintained under standard condition and with access to water and regular diet *ad libitum*.

Mice were weighed once a week and at the end of the experimental procedures were euthanized and their tissues surgically excised. Right femurs were dissected, fixed with 4% (vol/vol) paraformaldehyde for 18 hours at 4°C and processed for histological analysis. Left femurs were subjected to bone marrow flushing and then stored in liquid nitrogen for Western blot

and real-time PCR analysis. This animal interventional study is in accordance with the European Law Implementation of Directive 2010/63/EU and all experimental protocols were reviewed and approved by the Veterinary Department of the Italian Ministry of Health (Project 522-2016PR). Experimental procedures have been carried out following the standard biosecurity and the institutional safety procedures. Investigators were blinded to the group allocation. Power analysis: for α of 0.05 and $p < .05$; eight mice/group. Sample sizes were chosen based on pilot studies and prior related work.

Real-time PCR

Total RNA from mouse tissues was extracted using spin columns (Rneasy; Qiagen, Valencia, CA, USA) according to the manufacturer's instructions. Dnase I treatment was performed to remove genomic DNA contamination (Qiagen) and RNA integrity was assessed on agarose gels. Reverse transcription was performed using iScript Reverse Transcription Supermix (Bio-Rad Laboratories, Hercules, CA, USA). The resulting cDNA (20 ng) was subjected to quantitative PCR (qPCR) using the SsoFast EvaGreen Supermix (Bio-Rad Laboratories) on an Bio-Rad CFX96 Real-Time System (Bio-Rad Laboratories) for 40 cycles (denaturation 95°C for 5 s; annealing/extension 60°C for 10 s) after an initial 30-s step for enzyme activation at 95°C. To confirm the specificity of amplification products, the melting curve was performed between 65°C and 96°C, with 0.5°C incrementing every 10 s. Primers were designed by using Primer Blast (<https://www.ncbi.nlm.nih.gov/tools/primer-blast/>). We chose *Gapdh* as housekeeping gene because is stably expressed in bone. Primer sequences: *Gapdh* (S-acaccagtagactccacgaca, AS-acggcaattcaacggcacag); *Atf4* (S-gcctgactctgctgtacattac, AS-cacgggaaccactggagaag); *Sost* (S-tgctctactgcctacttg; AS-ggtctgcctcattctcc); *Dkk1* (S-aagttgaggttcgcgactcc; AS-gcaaacagcaaggctcagg); *Pdpr* (S-cgtcggaggatctctcattg; AS-agctcttttagggcagaacctt); *Gja1* (S-ctttcattgggggaaagcg; AS-ctgggacacctctcttctact); *Tfam* (S-taggcacgtattgcgtgag; AS-cagacaagactgatagacgaggg); *Bcl2* (S-tacgagtgggatgcttgag; AS-ggctggaaggaagatgc); and *Bax* (S-agatgaactggacagcaatag; AS-gcaaagtagaagagggaacc). All primers span an exon-exon junction. Each transcript was assayed in triplicate and quantitative measures were obtained using the $\Delta\Delta CT$ method and expressed as a fold change compared to control.

Western blotting

Thirty micrograms (30 μ g) of protein from cortical bone depleted from marrow and 20 μ g of protein from cell culture were solubilized with lysis buffer (50mM Tris (Tris(hydroxymethyl)aminomethane)-HCl (pH 8.0), 150mM HCl, 5mM ethylenediaminetetraacetic acid, 1% NP40, and 1mM phenylmethyl sulfonyl fluoride). The protein concentration was measured by DC Protein Assay (Bio-Rad Laboratories). Cell proteins were subjected to SDS-polyacrylamide gel electrophoresis (SDS-PAGE) and then transferred to nitrocellulose membranes (Millipore, Billerica, MA, USA). The blots were incubated overnight at 4°C using primary antibody anti-pERK (Santa Cruz Biotechnology, Santa Cruz, CA, USA), anti-Erk (Santa Cruz Biotechnology), β -Actin (Santa Cruz Biotechnology), anti-caspase-9 and anti-caspase-3 (Cell Signaling Technology, Beverly, MA, USA). Subsequently, membranes were incubated for 2 hours at room temperature with appropriate IRDye-labeled secondary antibodies (680/800 CW) (LI-COR Biosciences, Lincoln, NE, USA). For immunodetection, the Odyssey infrared imaging system was utilized (LI-COR Biosciences). All data were normalized to background and loading controls.

Histological analysis of cortical bone

Freshly dissected femurs were immediately fixed in ice-cold 4% paraformaldehyde solution for 18 hours. After decalcification, performed with 0.5M ethylenediaminetetraacetic acid (EDTA) at 4°C, bones were immersed in 20% sucrose and 2% polyvinylpyrrolidone (PVP) solution for 24 hours. Femurs were then embedded and frozen in optimal cutting temperature (OCT) compound (VWR Chemicals). For histological analyses, sections were generated by using a SLEE MEV Semi-Automatic Cryostat (SLEE medical GmbH, Mainz, Germany).

For the analysis of osteocytes and empty lacunae, three sections per sample and five high-power fields for each section were analyzed. Five-micrometer-thick (5- μ m-thick) histological sections were cut and stained with hematoxylin and eosin (H&E). Histological sections were viewed under a Nikon Eclipse 80i light microscope (Nikon) using a 40 \times objective lens. Images were taken at 150 dpi (3840 \times 3072 pixels) and analyzed by using ImageJ software (NIH, Bethesda, MD, USA; <https://imagej.nih.gov/ij/>), by manually outlining bone surface.

Immunofluorescence and laser confocal microscopy

MLO-Y4 cells were fixed in 4% paraformaldehyde in PBS for 10 min and permeabilized with Triton X-100 0.5% in PBS for 10 min at room temperature (RT) and incubated with blocking buffer (PBS, pH 7.4, 2% bovine serum albumin, and 0.1% Triton X-100) in PBS for 30 min at RT to prevent nonspecific interactions. Then, MLO-Y4 cells were incubated with primary antibody against caspase-3 (Cell Signaling Technology) and cleaved caspase-3 (Cell Signaling Technology) for 2 hours at 37°C revealed by appropriate fluorophore-conjugated secondary antibody (Alexa Fluor-555 and Alexa Fluor-488; Invitrogen, Carlsbad, CA, USA) for 1 hour at RT, and then counterstained with TO-PRO-3 (Invitrogen) diluted 1:10⁴ in PBS for 15 min. Finally, the cells were coverslipped with ProLong Diamond Antifade Mountant (Life Technologies Corporation, Eugene, OR, USA) and examined under a Leica TCS SP5 confocal laser scanning microscope (Leica Microsystems, Mannheim, Germany) using a sequential scan procedure. Confocal images were taken at 0.2- μ m intervals through the z axis by 40 \times and 20 \times objective lens with either 1 \times or 2 \times zoom factors. Z-stacks of serial optical planes (projection images) and single optical planes were analyzed, digitally recorded, and stored as TIFF files using Adobe Photoshop software (Adobe Systems, Inc., San Jose, CA, USA). Fluorescence intensity analysis was performed using Adobe Photoshop software (Adobe Systems, Inc.).

Statistical analysis

Data were analyzed using two-tailed Student's *t* test when two groups were compared. ANOVA was used when more than two groups were compared, followed by Tukey's post hoc analysis to compare the groups. Values were considered statistically significant at $p < .05$. Experiments were repeated at least three times as biological replicates, with two to three technical replicates. All quantitative data are presented as mean \pm SE.

Results

Irisin increases *Atf4* expression in MLO-Y4 osteocytes through Erk1/Erk2 activation

We have previously reported that irisin stimulated the phosphorylation of mitogen-activated protein kinases (MAPKs) Erk1 and Erk2 (pErk) and induced a rapid upregulation of the transcription factor

Atf4 in bone marrow osteoblasts.⁽¹³⁾ Here we sought to investigate the effect of irisin on osteocytes *in vitro*. Incubation with rec-irisin (100 ng/mL) in MLO-Y4 cells activates Erk phosphorylation within 5 min of application, as also shown by densitometric analysis (Fig. 1A). Gene expression analysis showed that irisin also induced a rapid upregulation of the transcription factor *Atf4* within 8 hours (2.5-fold, $p < .05$) (Fig. 1B). Irisin-induced upregulation of *Atf4* mRNA was prevented by inhibiting pErk activation using 50 μ M PD98059 pretreatment (Fig. 1B), suggesting that the effect of irisin on this transcription factor occurs through an Erk-dependent pathway in MLO-Y4 osteocytes (Fig. 1C).

Effects of irisin on MLO-Y4 cells depending on the mode of exposure

Figure 2 summarizes the effects of rec-irisin (100 ng/mL) on the expression of some master genes of osteocytes after repeating the continuous or intermittent exposure to the myokine three times in each 48-hour incubation cycle. In Fig. 2A, we show that 6 days' exposure to rec-irisin was effective in upregulating *Atf4* mRNA expression with a greater effect when MLO-Y4 cells were continuously treated (ninefold, $p < .05$) than intermittently treated (4.5-fold, $p < .05$) (Fig. 2B). Although intermittent pulses of 8 hours and 24 hours showed a nonsignificant tendency to increase, the effect of irisin on *Atf4* mRNA does not appear to depend on the mode of irisin

exposure. Conversely, *Sost* mRNA was severely downregulated only upon intermittent irisin administration (10-fold) after 3-hour ($p < .01$), 8-hour ($p < .01$) and 24-hour pulses ($p < .001$) (Fig. 2D), whereas continuous irisin exposure did not modify its expression (Fig. 2C).

Contrastingly, mRNA levels of *Dkk1*, the other antagonist of the Wnt/beta-catenin signaling pathway, were downregulated by rec-irisin when continuously administered (1.5-fold, $p < .05$) (Fig. 2E) and also with the shortest pulses of intermittent rec-irisin (3 hours) (3.5-fold, $p < .05$) (Fig. 2F). We also found that irisin modulates mRNA expression of two osteocyte genes. Interestingly, Podoplanin (*Pdpn*), a protein essential during the formation of dendritic processes, was upregulated upon continuous irisin administration (2.5-fold, $p < .05$) (Fig. 2G, while not significantly modulated by intermittent treatment (Fig. 2H)). Connexin 43 (*Gja1*), a protein forming gap junction channels and hemichannels in osteocytes, increased after both continuous (5.7-fold, $p < .001$) (Fig. 2I) and the longest intermittent pulses (24 hours) of irisin administration (2.3-fold, $p < .01$) (Fig. 2J).

Irisin inhibits apoptosis modulating caspase-9 and caspase-3 expression in MLO-Y4 cells

We have previously shown that treatment with rec-irisin *in vivo* increased the gene expression of mitochondrial transcription

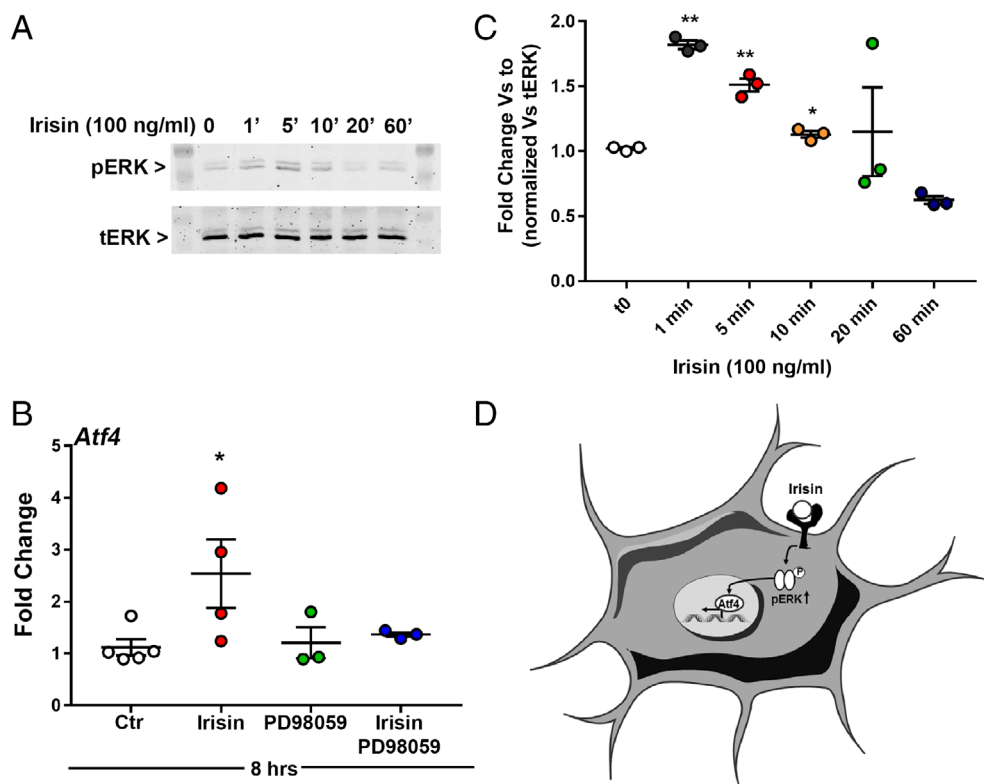


Fig. 1. Irisin increases *Atf4* expression in MLO-Y4 osteocytes through Erk1/Erk2 activation (A) Western immunoblotting and densitometric analysis showing Erk phosphorylation (pErk) triggered by rec-irisin (100 ng/mL) in MLO-Y4 osteocyte cultures (representative Western blot image of $n = 3$ independent experiments). (B) Quantitative PCR showing upregulation of *Atf4* mRNA expression after 8 hours of treatment with 100 ng/mL rec-irisin, but no effect inhibiting pErk activation with 50 μ M PD98059 pre-treatment. *Atf4* mRNA expression was normalized to *Gapdh* and plotted as fold-increase from the non-treated (control) sample ($n = 3$ independent experiments). ANOVA followed by Tukey's post hoc analysis was used to compare treatments. Data are presented as mean \pm SE. * $p < .05$. (C) Schematic representation of irisin's action on osteocytes to activate ERK phosphorylation, which in turn stimulates the increase of *Atf4* mRNA levels.

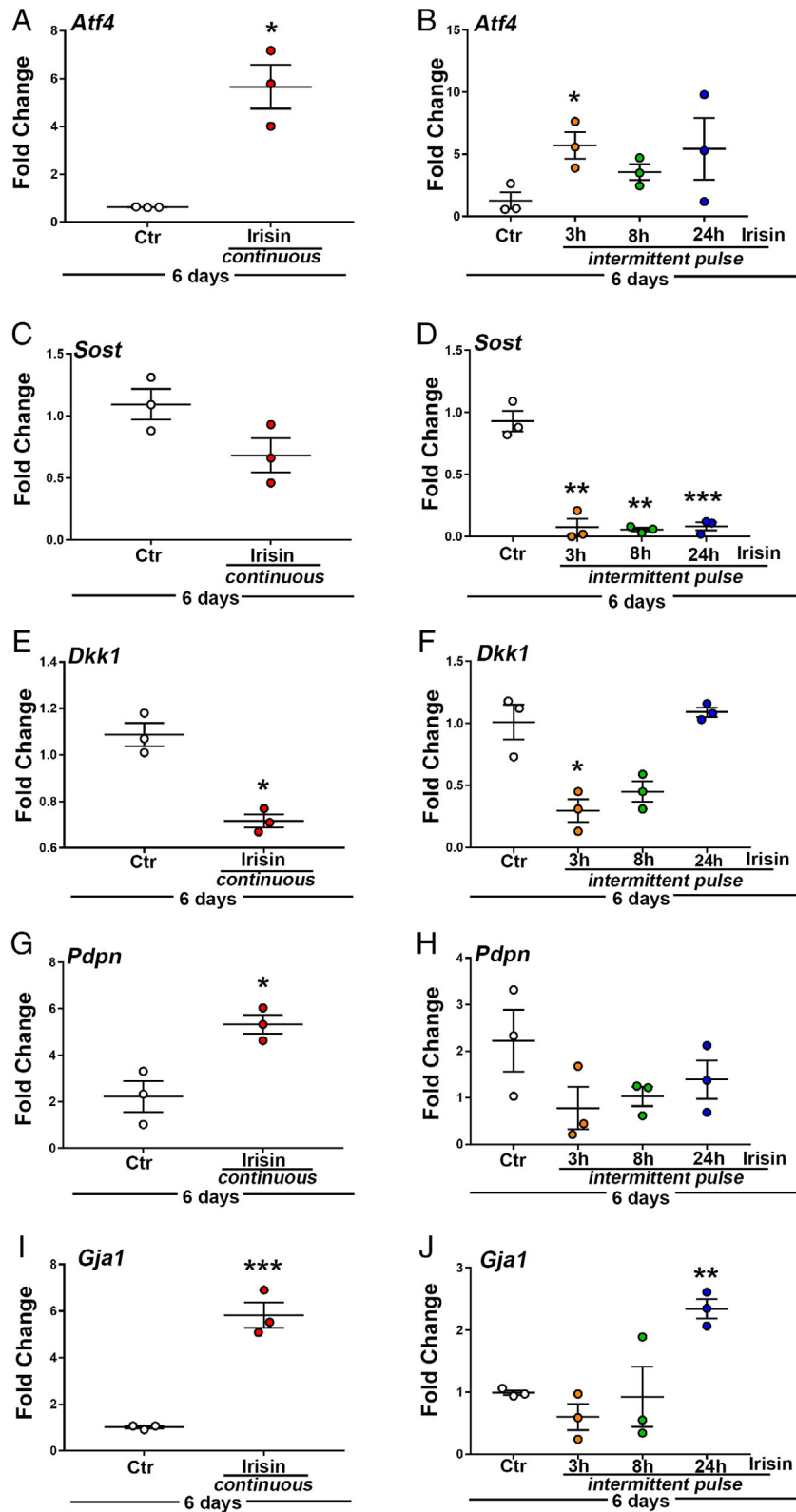


Fig. 2. Effects of irisin on MLO-Y4 cells depending on the mode of exposure figure 2 shows the effects of rec-irisin (100 ng/mL) on the expression of some master genes of MLO-Y4 osteocytes after repeating 3 times the continuous or intermittent exposure to the myokine in each 48-hours incubation cycle (6-day treatment). (A,C,E,G,I) mRNA expression levels of *Atf4*, *Sost*, *Dkk1*, *Pdpn*, and *Gja1* were assayed (qPCR) after 6-day culture with rec-irisin refreshed every 48 hours (continuous protocol). (B,D,F,H,J) mRNA expression levels of *Atf4*, *Sost*, *Dkk1*, *Pdpn*, and *Gja1* were assayed (qPCR) after 6-day culture with rec-irisin added for 3-hour, 8-hour, or 24-hour pulses. After each treatment-pulse, the medium was changed, and the procedure repeated every 48 hours for three times (intermittent protocol). Gene expression was normalized to *Gapdh* and plotted as fold-increase from the nontreated (control) sample ($n = 3$ independent experiments). Unpaired Student's *t* test and ANOVA, followed by Tukey's post hoc analysis, were used to compare treatments. Data are presented as mean \pm SE. * $p < .05$, ** $p < .01$, *** $p < .001$.

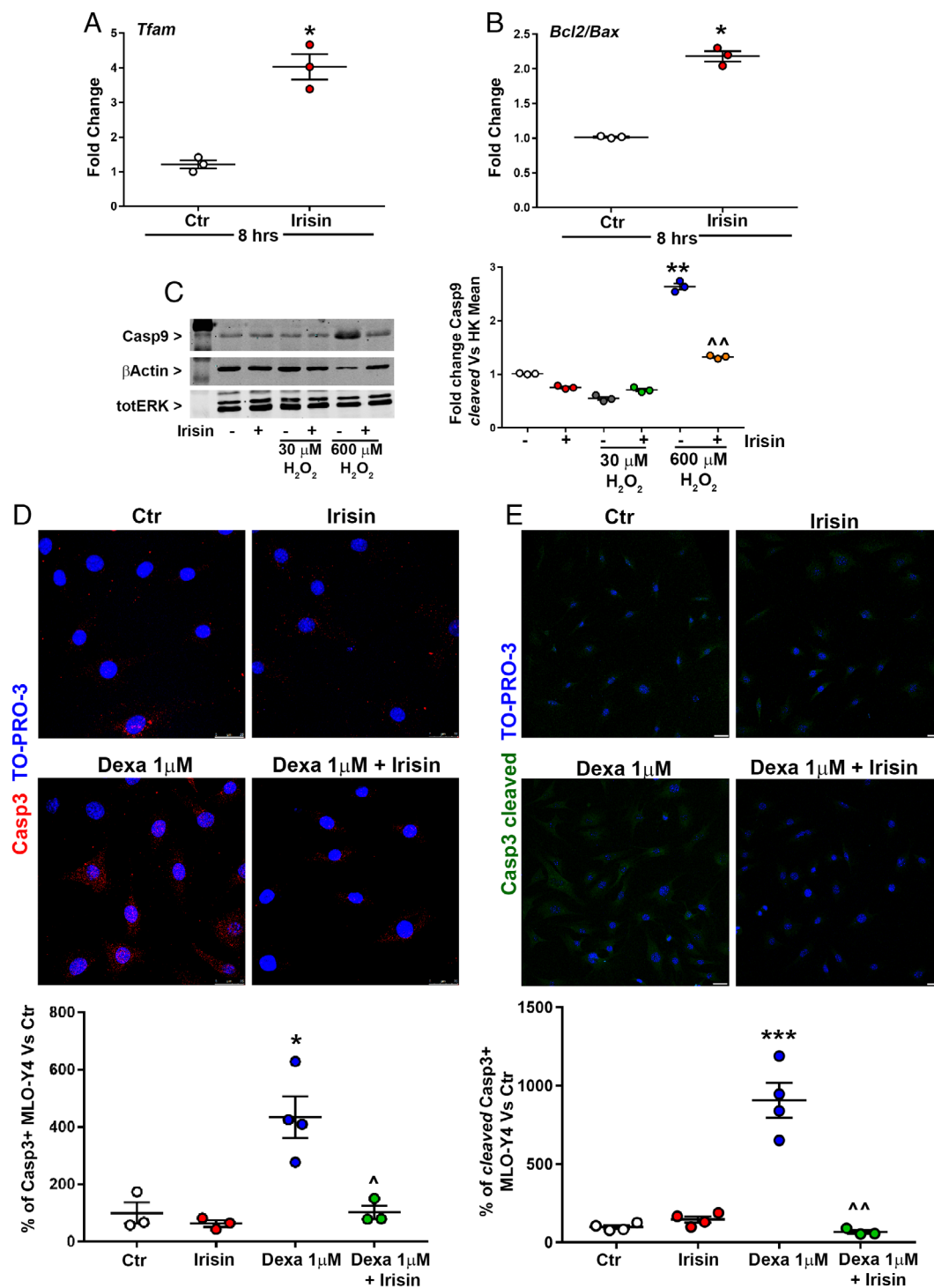


Fig. 3. Irisin inhibits apoptosis modulating caspase-9 and caspase-3 expression in MLO-Y4 cells quantitative PCR showing upregulation of mRNAs for (A) *Tfam* and (B) *Bcl2/Bax* ratio after 8 hours of treatment with 100 ng/mL rec-irisin in MLO-Y4 osteocytes. Gene expression was normalized to *Gapdh* and plotted as fold-increase from the nontreated (control) sample ($n = 3$ independent experiments). (C) Western immunoblotting and densitometric analysis of caspase-9 in MLO-Y4 osteocytes pretreated with 30 μ M or 600 μ M of H₂O₂ for 2 hours and then treated with rec-irisin (100 ng/mL) for 24 hours (representative Western blot image of $n = 3$ independent experiments). Normalization was performed on the mean of two housekeeping proteins (HK). (D) Representative confocal images and quantification of MLO-Y4 osteocytes immunolabeled for caspase-3 (red). Dexa 1 μ M + irisin-treated cells showing a reduced caspase-3 (red) expression compared to Dexa 1 μ M-treated cells. Nuclei counterstained with TO-PRO-3 (blue). Magnification $\times 40$. Scale bar = 25 μ m. (E) Representative confocal images and quantification of MLO-Y4 osteocytes immunolabeled for cleaved caspase-3 (green). Dexa 1 μ M + irisin-treated cells showing a reduced cleaved caspase-3 (green) expression compared to Dexa 1 μ M-treated cells. Nuclei counterstained with TO-PRO-3 (blue). Magnification: $\times 20$. Scale bar = 25 μ m. ANOVA followed by Tukey's post hoc analysis was used to compare treatments. Data are presented as mean \pm SE. *** $p < .001$, * $p < .05$ versus Ctr; ^ $p < .01$, ^ $p < .05$ versus dexamethasone 1 μ M. Dexa = dexamethasone; Ctr = control.

factor A (*Tfam*) in skeletal muscle of unloaded mice.⁽¹⁰⁾ Here we found that short treatment (8 hours) with rec-irisin increased the expression of *Tfam* (fourfold, $p < .05$) (Fig. 3A) and upregulated the pro-survival Bcl2/Bax ratio (twofold, $p < .05$) (Fig. 3B) in MLO-Y4 cells. Because *Tfam* is a key regulator in the

mitochondrial pathway of cell death,⁽¹⁴⁾ and the Bcl-2 family of proteins regulate apoptosis by controlling mitochondrial permeability,⁽¹⁵⁾ we next investigated whether the expression of caspases was modulated by irisin in osteocytes. By pretreating MLO-Y4 cells with either a low (30 μ M) or high (600 μ M)

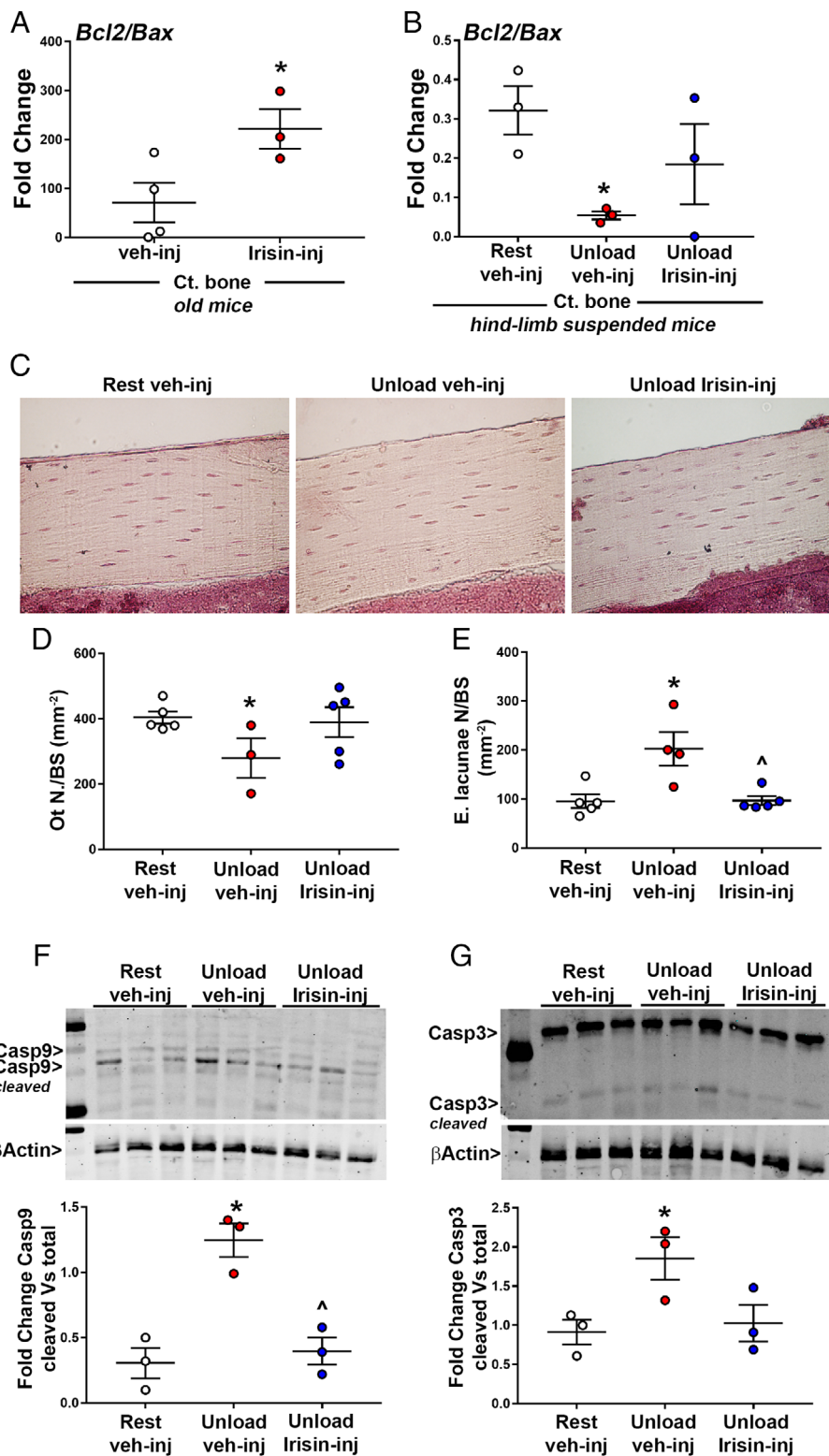


Fig. 4. Legend on next page.

concentration of H₂O₂ for 2 hours, followed by 24-hour treatment with rec-irisin, we observed that the increase of caspase-9 after high H₂O₂ stimulation was fully reversed by irisin treatment (Fig. 3C). Using immunofluorescence staining in MLO-Y4 cells, we showed that the increased cleavage of caspase-3 induced by 1 μM dexamethasone (ninefold, $p < .001$) was completely inhibited by 24-hour treatment with rec-irisin (Fig. 3E), in parallel to the inhibition of increased caspase-3 expression (4.3-fold, $p < .05$) (Fig. 3D).

Irisin prevents osteocyte apoptosis and caspase-9 and caspase-3 activation during unloading

We next investigated whether irisin treatment exerted pro-survival action in cortical bone of osteoporotic murine models treated with 100 μg/kg rec-irisin once a week for 4 weeks. In femurs of 18-month-old mice treated with irisin, we observed a threefold increase ($p < .05$) of Bcl2/Bax ratio compared with mice treated with vehicle (Fig. 4A). Likewise, in hindlimb-suspended mice, the expected decrease of Bcl2/Bax ratio (6.4-fold, $p < .05$ versus rest veh-inj) observed in cortical bone of mice treated with vehicle (unload veh-inj), was partially prevented by irisin treatment ($p = .57$ versus rest veh-inj; $p = .42$ versus unload veh-inj) (Fig. 4B). Earlier study from our group clearly demonstrated that irisin treatment was effective in preventing bone loss during unloading.⁽¹⁰⁾ Following this evidence, we proceeded to determine whether irisin influences osteocyte function by preserving their survival in the absence of load. As shown in Fig. 4C, H&E staining revealed that osteocyte number (Ot N) per bone surface (BS) was reduced by ~30% ($p < .05$) in unloaded mice injected with vehicle compared to control mice, whereas rec-irisin treatment partially protected osteocytes from cell death ($p = .78$ versus rest veh-inj; $p = .19$ versus unload veh-inj) (Fig. 4D). Reliably, the increase of empty lacunae (*E. lacunae* N) per BS in unloaded mice treated with vehicle (+111%; $p < .05$ versus rest veh-inj), was inhibited by irisin ($p = .94$ versus rest veh-inj; $p < .05$ versus unload veh-inj) (Fig. 4E).

The intrinsic apoptotic pathway, strictly controlled by the Bcl2 family of proteins, mainly leads to the activation of caspase-9, which in turn cleaves and activates the executioner caspase-3.⁽¹⁶⁾ In order to determine whether irisin protects from osteocyte death by preventing caspase activation also in vivo, we analyzed their cleavage in cortical bone of unloaded mice. By densitometric analysis, we detected a fourfold increase of cleaved caspase-9 in unloaded mice treated with vehicle ($p < .05$ versus rest veh-inj), whereas the cleavage was completely inhibited by rec-irisin treatment ($p < .05$ versus rest

veh-inj; $p < .05$ versus unload veh-inj) (Fig. 4F). Although disuse-induced activation of caspase-3 was less marked than caspase-9, we found that irisin slightly reduced its cleavage ($p < .05$ versus rest veh-inj; $p = .08$ versus unload veh-inj) (Fig. 4G).

Discussion

The aim of our study was to determine the effects of rec-irisin on osteocyte function and survival. Numerous works by us and other groups have shown that irisin targets bone tissue mainly by increasing osteoblast differentiation and activity,^(9,17–19) but new recent findings have proved that irisin also acts on osteocytes via integrin αV/β5 receptor activating phosphorylation of focal adhesion kinase (FAK) and cyclic AMP response element-binding protein (CREB).⁽⁸⁾ In the present study, we show that irisin treatment in MLO-Y4 osteocytes rapidly activates phosphorylation of Erk1/Erk2 after only 5 min and increases *Atf4* mRNA expression after 8 hours of treatment. The irisin-mediated *Atf4* upregulation occurs through Erk1/Erk2 phosphorylation (pERK) because it is inhibited by pretreatment with a selective inhibitor of MAP kinase kinases (MAPKK), thereby preventing the activation of its downstream molecule ERK. Although other transcription factors including Runx-related transcription factor 2 (Runx2) and Osterix are implicated in the anabolic actions of irisin in osteoblasts,⁽⁹⁾ our previous studies have clearly shown that irisin acts on *Atf4* by directly increasing its expression.^(9,17) *Atf4* is a well-established regulator of bone development⁽²⁰⁾ and a critical transcription factor for proliferation, differentiation, and survival in osteoblasts.^(21,22) However, Yu and colleagues⁽²³⁾ showed that *Atf4* is also essential in osteocytes for PTH-mediated inhibition of apoptosis, because this effect was completely abolished in cortical osteocytes from *Atf4* knockout mice treated with PTH.

Our data also showed that *Atf4* mRNA expression increased in MLO-Y4 osteocytes after a longer exposure to irisin, either continuously administered or given with intermittent short pulses. Although there was a greater effect following continuous treatment, *Atf4* modulation did not appear to be strictly dependent on the mode of irisin exposure. On the contrary, the gene expression of the bone inhibitor sclerostin, *Sost*, was severely downregulated in MLO-Y4 osteocytes only upon intermittent irisin administration, whereas continuous irisin exposure did not modify its expression. These findings are consistent with our previous report of intermittent treatment with irisin in hindlimb-suspended mice, in which 4 weeks of 100-μg/kg rec-irisin treatment, given once a week, decreased sclerostin levels in cortical bone respect to hindlimb-suspended mice treated with vehicle.

FIG. 4 Irisin prevents osteocyte apoptosis and caspase-9 and caspase-3 activation during unloading quantitative PCR showing upregulation of *Bcl2/Bax* ratio in cortical bone, depleted of marrow, of (A) 18-month-old mice and (B) 2-month-old hindlimb-suspended mice treated with vehicle or 100 μg/kg rec-irisin once a week for 4 weeks, euthanized 24 hours after last dose. Gene expression was normalized to *Gapdh* and plotted as fold-increase from the veh-injected (control) mice ($n = 5–6$ mice per group). (C) Photomicrographs of hematoxylin and eosin-stained sections of femurs from rest vehicle-injected and unload vehicle-injected or irisin-injected mice (magnification: ×40). (D) Quantitative assessments of osteocyte number per bone surface (Ot N./BS) and (E) empty lacunae per bone surface (*E. lacunae* N./BS) in cortical bone of femurs from normal loading mice (rest vehicle-inj) and unloaded mice treated with vehicle or rec-irisin ($n = 6$ to 7 mice per group). (F) Western immunoblotting and densitometric quantitation of total and cleaved caspase-9 and (G) caspase-3 expressions in cortical bone, depleted of marrow, of 2-month-old hindlimb-suspended mice treated with vehicle or 100 μg/kg rec-irisin once a week for 4 weeks. First, expressions of total caspase-9 and caspase-3 were normalized to control loading (β-Actin). Subsequently, expressions of cleaved caspase-9 and caspase-3 were normalized to the respective total caspase and then plotted as fold-increase from the veh-injected (control) mice ($n = 3$ mice per group). ANOVA followed by Tukey's post hoc analysis was used to compare treatments. Data are presented as mean ± SE. * $p < .05$ versus rest veh-inj mice, † $p < .05$ versus unload veh-inj mice.

The finding that *Sost* modulation is strictly dependent on irisin's mode of exposure to osteocytes could explain the apparent contradiction with results obtained by Kim and colleagues.⁽⁸⁾ Indeed, authors have recently showed that a continuous treatment with a high dose (1 mg/kg) of irisin by daily injection for 6 days raised *Sost* mRNA levels in cortical bone of mice.⁽⁸⁾

Albeit to a lesser extent than *Sost*, the other antagonist of the Wnt/beta-catenin signaling pathway, *Dkk1*,⁽¹⁾ was also downregulated by rec-irisin in MLO-Y4 osteocytes with a greater effect when it was administered intermittently with very short pulses (3 hours) than continuously (3.5-fold versus 1.5-fold). To our knowledge, this is the first in vitro evidence showing a direct action of irisin on *Dkk1* expression in osteocytes. Consistently, we have previously observed a negative association between serum levels of irisin and DKK1 in a population of healthy children aged 7 to 13 years, thus supporting the positive link of irisin with bone status in these children.⁽²⁴⁾

To further investigate the role of irisin on osteocyte function, we also evaluated the expression of two osteocyte marker genes, *Pdpr* and *Gja1*. *Pdpr*, also known as E11/gp38, is a glycoprotein expressed mainly in newly embedded osteocytes. In vitro and in vivo studies have shown that *Pdpr* is crucial for dendrite formation and development of a normal osteocyte canalicular network. Deletion of *Pdpr* with siRNAs in MLO-Y4 cells inhibited dendrite formation⁽²⁵⁾ and *Pdpr* conditional knockout mice displayed a compromised osteocyte dendrite elongation and impaired bone microarchitecture.⁽²⁶⁾ Here we found that 6 days of continuous treatment with rec-irisin increased *Pdpr* mRNA expression, thus suggesting that this myokine stimulates dendrite formation in osteocytes. Further studies are needed to confirm whether this effect also occurs in vivo, thus supporting the hypothesis that irisin increases cortical bone mass⁽⁹⁾ also by improving the development of a normal osteocyte canalicular network.

Dendritic processes of osteocytes form this network connecting neighboring osteocytes and cells on the bone surface through gap junction channels formed by *Gja1*.⁽²⁷⁾ Previous in vitro studies revealed that *Gja1* hemichannels in osteocytes are highly responsive to mechanical loading^(28–30) and are involved in the transduction of anti-apoptotic signals.⁽³¹⁾ We observed here the significant increase of mRNA levels for *Gja1* in MLO-Y4 osteocytes treated either continuously or with the longest intermittent pulses (24 hours) of rec-irisin administration. Thus, it is possible that irisin-induced increase of *Gja1* hemichannels expression may contribute to the osteocyte response to mechanical loading because this myokine mainly acts as a biochemical messenger between muscle and bone in the presence of load.

Previous data have shown that irisin treatment reduced hydrogen peroxide-induced apoptosis in MLO-Y4 cells.⁽⁸⁾ Our study aimed to understand which signaling pathway, the extrinsic or the intrinsic pathway, both converging on the activation of the caspase protease family,⁽³²⁾ is engaged by irisin to promote the survival of osteocytes in bone tissue. Massive apoptosis has been observed in *Tfam* knockout embryos, suggesting that this transcription factor might be a key regulator in preventing activation of the mitochondrial pathway of cell death.⁽¹⁴⁾ In addition, our previous findings showed that irisin treatment in vivo increased mitochondrial biogenesis and upregulated the expression of the mitochondrial transcription factor *Tfam* in atrophic skeletal muscle.⁽¹⁰⁾ This led us to hypothesize that irisin might have been primarily involved in the mitochondrial (intrinsic) pathway. Consistently, here we found that irisin increased the expression of *Tfam* and upregulated the pro-survival Bcl2/Bax ratio in MLO-Y4 osteocytes, particularly by enhancing the expression of *Bcl2* mRNA. Proteins of the Bcl-2 family regulate the mitochondrial

pathway of apoptosis by controlling the permeabilization of the outer mitochondrial membrane.⁽¹⁵⁾ High expression of Bcl-2 blocks cell death by preventing the activation and homo-oligomerization of Bax, which participates in forming pores in the outer mitochondrial membrane, leading to the release of the contents of the mitochondrial intermembrane space into the cytoplasm.⁽³³⁾ Once released from mitochondria during apoptosis, Cytochrome c binds to a cytosolic protein (Apaf-1) containing a caspase-recruitment domain (CARD) to form the apoptosome and subsequently to recruit multiple procaspase-9 molecules, facilitating their autoactivation. In turn, the caspase-9 bound to the apoptosome cleaves and activates downstream executioner caspases such as caspase-3.⁽³³⁾

We, therefore, sought to investigate whether caspases were modulated by irisin in osteocytes. By inducing apoptosis in MLO-Y4 cells with 2 hours of pretreatment with 600µM H₂O₂, we observed that the increase of caspase-9 after 24 hours was prevented in osteocytes cultured in the presence of irisin. In addition, the increased cleavage of caspase-3 after a longer exposure to the pro-apoptotic agent dexamethasone was inhibited by the treatment with irisin. Next, we performed in vivo analysis in a murine model of osteoporosis that allowed us to evaluate whether irisin prevented bone damage also acting on osteocyte viability by controlling activation of caspases. First, we measured the Bcl2/Bax ratio in femurs of old mice and unloaded mice. As for MLO-Y4 cells, we find in cortical bone of these mice a significant pro-survival stimulus given by irisin, with a more pronounced effect on the Bcl2/Bax ratio in unloaded mice. As expected, the unloading condition caused a reduction in the osteocyte number and an increase in empty lacunae, which are hallmarks of cell death. However, mice treated with irisin during the hindlimb suspension were partially protected from cortical osteocyte death. Interestingly, both osteocyte and empty lacunae numbers were comparable to those of a mouse kept under normal loading conditions. Moreover, our findings showed that irisin preserves osteocyte viability in the absence of load by preventing the activation of caspase-9, and, although much less marked than caspase-9, the unloading-induced activation of caspase-3 was slightly prevented by irisin treatment.

In conclusion, in this study, we show that irisin acts on osteocyte via activation of ERKs and new gene transcription. Of note, our results suggest that irisin has to be administered at low dose and intermittently in order to gain an anabolic effect on bone by decreasing sclerostin. As for PTH, which exerts both catabolic and anabolic effects on the skeleton depending on the mode of administration,⁽³⁴⁾ chronic high irisin levels could lead to bone catabolism, while lower and intermittent irisin pulses, as occurs during exercise, promote bone anabolism, leading to a favorable skeletal outcome.⁽⁹⁾

Furthermore, the survival responses triggered by irisin, which is a loading-mimetic molecule, provides evidence for its contribution to the response of osteocytes to both biochemical and physical stimuli. Together, besides its role in stimulating osteoblast differentiation and activity, this study further corroborates the work by Kim and colleagues,⁽⁸⁾ showing irisin's mechanism of action in protecting osteocytes against cell death. Considering that osteocytes do not divide or differentiate in vivo, preservation of osteocyte viability is likely to be one of the most relevant biological responses for maintaining bone mass and function.

Disclosures

As stated here, there are no potential conflicts of interest for all authors. All authors approved the final version of the submitted

manuscript and agree to be accountable for all aspects of the work in ensuring that questions related to the accuracy or integrity of any part of the work are appropriately investigated and resolved.

Acknowledgments

This work was supported in part by MIUR grant ex60% (to MG), by SIOMMMS grant (to GC), and by ERISTO (ESA) grant (to MG).

Authors' roles: Study design: GS, GC, GP, and MG. Study conduct: GS, GC, and LL. Data collection: GS and GC. Data analysis: GS and LS. Data interpretation: GS, GC, LS, LL, GB, ME, SC, GP, and MG. Drafting manuscript: GS, GC, GP, and MG. Revising manuscript content: ME and SC. Approving final version of manuscript: GS, GC, LS, LL, GB, ME, SC, GP, and MG. MG takes responsibility for the integrity of the data analysis.

References

1. Bonewald LF. The amazing osteocyte. *J Bone Miner Res.* 2011;26(2):229–38.
2. Tomkinson A, Reeve J, Shaw RW, Noble BS. The death of osteocytes via apoptosis accompanies estrogen withdrawal in human bone. *J Clin Endocrinol Metab.* 1997;82:3128–35.
3. Weinstein RS, Jilka RL, Parfitt AM, Manolagas SC. Inhibition of osteoblastogenesis and promotion of apoptosis of osteoblasts and osteocytes by glucocorticoids: potential mechanisms of their deleterious effects on bone. *J Clin Invest.* 1998;102:274–82.
4. Cabahug-Zuckerman P, Frikha-Benayed D, Majeska RJ, et al. Osteocyte apoptosis caused by hindlimb unloading is required to trigger osteocyte RANKL production and subsequent resorption of cortical and trabecular bone in mice femurs. *J Bone Miner Res.* 2016;31(7):1356–65.
5. Jilka RL, Weinstein RS, Bellido T, Roberson P, Parfitt AM, Manolagas SC. Increased bone formation by prevention of osteoblast apoptosis with parathyroid hormone. *J Clin Invest.* 1999;104:439–46.
6. Plotkin LI, Weinstein RS, Parfitt AM, Roberson PK, Manolagas SC, Bellido T. Prevention of osteocyte and osteoblast apoptosis by bisphosphonates and calcitonin. *J Clin Invest.* 1999;104:1363–74.
7. Kitase Y, Vallejo JA, Guthel W, et al. Beta-aminoisobutyric acid, 1-BAIBA, is a muscle-derived osteocyte survival factor. *Cell Rep.* 2018;22(6):1531–44.
8. Kim H, Wrann CD, Jedrychowski M, et al. Irisin mediates effects on bone and fat via α v integrin receptors. *Cell.* 2018;175:1756–68.e17.
9. Colaianni G, Cuscito C, Mongelli T, et al. The myokine irisin increases cortical bone mass. *Proc Natl Acad Sci U S A.* 2015;112:12157–62.
10. Colaianni G, Mongelli T, Cuscito C, et al. Irisin prevents and restores bone loss and muscle atrophy in hind-limb suspended mice. *Sci Rep.* 2017;7:2811.
11. Kato Y, Windle JJ, Koop BA, Mundy GR, Bonewald LF. Establishment of an osteocyte-like cell line, MLO-Y4. *J Bone Miner Res.* 1997;12:2014–23.
12. Wronski TJ, Morey-Holton ER. Skeletal response to simulated weightlessness: a comparison of suspension techniques. *Aviat Space Environ Med.* 1987;58(1):63–8.
13. Palermo A, Strollo R, Maddaloni E, et al. Irisin is associated with osteoporotic fractures independently of bone mineral density, body composition or daily physical activity. *Clin Endocrinol.* 2015;82:615–9.
14. Larsson NG, Wang J, Wilhelmsson H, et al. Mitochondrial transcription factor a is necessary for mtDNA maintenance and embryogenesis in mice. *Nat Genet.* 1998;18:231–6.
15. Brunelle JK, Letai A. Control of mitochondrial apoptosis by the Bcl-2 family. *J Cell Sci.* 2009;122:437–41.
16. Fesik SW. Insights into programmed cell through structural biology. *Cell.* 2000;103(2):273–82.
17. Colanianni G, Cuscito C, Mongelli T, et al. Irisin enhances osteoblast differentiation in vitro. *Int J Endocrinol.* 2014;2014:902186. <https://doi.org/10.1155/2014/902186>.
18. Holmes D. Bone: irisin boosts bone mass. *Nat Rev Endocrinol.* 2015;12:689.
19. Yong Qiao X, Nie Y, Xian Ma Y, et al. Irisin promotes osteoblast proliferation and differentiation via activating the MAP kinase signaling pathways. *Sci Rep.* 2016;6:18732.
20. Yang X, Matsuda K, Bialek P, et al. ATF4 is a substrate of RSK2 and an essential regulator of osteoblast biology; implication for Coffin-Lowry syndrome. *Cell.* 2004;117:387–98.
21. Yang X, Karsenty G. ATF4, the osteoblast accumulation of which is determined post-translationally, can induce osteoblast-specific gene expression in non-osteoblastic cells. *J Biol Chem.* 2004;279:47109–14.
22. Zhang X, Yu S, Galson DL, et al. Activating transcription factor 4 is critical for proliferation and survival in primary bone marrow stromal cells and calvarial osteoblasts. *J Cell Biochem.* 2008;105:885–95.
23. Yu S, Franceschi RT, Luo M, et al. Critical role of activating transcription factor 4 in the anabolic actions of parathyroid hormone in bone. *PLoS One.* 2009;4:e7583.
24. Colaianni G, Faienza MF, Sanesi L, et al. Irisin serum levels positively correlate with bone mineral status in a population of healthy children. *Pediatr Res.* 2019;85:484–8.
25. Zhang K, Barragan-Adjemian C, Ye L, et al. E11/gp38 selective expression in osteocytes: regulation by mechanical strain and role in dendrite elongation. *Mol Cell Biol.* 2006;26:4539–52.
26. Staines KA, Javaheri B, Hohenstein P, et al. Hypomorphic conditional deletion of E11/Podoplanin reveals a role in osteocyte dendrite elongation. *J Cell Physiol.* 2017;232:3006–19.
27. Bonewald LF. Generation and function of osteocyte dendritic processes. *J Musculoskelet Neuronal Interact.* 2005;5:321–4.
28. Cherian PP, Siller-Jackson AJ, Gu S, et al. Mechanical strain opens connexin 43 hemichannels in osteocytes: a novel mechanism for the release of prostaglandin. *Mol Biol Cell.* 2005;16:3100–6.
29. Genetos DC, Kephart CJ, Zhang Y, Yellowley CE, Donahue HJ. Oscillating fluid flow activation of gap junction hemichannels induces ATP release from MLO-Y4 osteocytes. *J Cell Physiol.* 2007;212:207–14.
30. Siller-Jackson AJ, Burra S, Gu S, et al. Adaptation of connexin 43-hemichannel prostaglandin release to mechanical loading. *J Biol Chem.* 2008;283:26374–82.
31. Plotkin LI, Manolagas SC, Bellido T. Transduction of cell survival signals by connexin-43 hemichannels. *J Biol Chem.* 2002;277:8648–57.
32. Green DR, Llambi F. Cell death signaling. *Cold Spring Harb Perspect Biol.* 2015;7(12):a006080.
33. Wang X. The expanding role of mitochondria in apoptosis. *Genes Dev.* 2001;15:2922–33.
34. Silva BC, Costa AG, Cusano NE, Kousteni S, Bilezikian JP. Catabolic and anabolic actions of parathyroid hormone on the skeleton. *J Endocrinol Invest.* 2011;34:801–10.